Strain effects on basal-plane hydrogenation of graphene: A first-principles study

Kun Xue[1] and Zhiping Xu[2,a)]
[1]*State Key Laboratory of Explosion Science and Technology, Beijing Institute of Technology, Beijing 100081, People's Republic of China*
[2]*Department of Civil and Environmental Engineering, Massachusetts Institute of Technology, Cambridge, 02139 Massachusetts, USA*

(Received 15 December 2009; accepted 4 January 2010; published online 9 February 2010)

In this letter we discuss basal-plane hydrogenation of graphene, in the extent of intercoupling between strain and electronic structure. Our first-principles calculations reveal that the atomic structures, binding energies, mechanical and electronic properties of graphene are significantly modified by applying strain. At a biaxial strain of 10%, binding energies of hydrogen on graphene can be improved by 53.89% and 23.56% in the *symmetric* and *antisymmetric* phase. In symmetric phase, carbon-hydrogen binding is unstable in compression. In antisymmetric phase, binding of hydrogen atoms reduces the sp^2 characteristic of graphene, which is partially recovered at finite tensile strain. © *2010 American Institute of Physics*. [doi:10.1063/1.3298552]

Graphene, the ultimately monoatomically layered material, possesses fascinating properties. It is amiable to molecular functionalization[1,2] and planar processing.[3] Recently there are arising efforts in the physical chemistry of graphene, especially in the extent of molecular doping and gas sensoring.[1] The notion of doping has been renovated in a reversible manner thanks to the coexistence chemical inertness of sp^2 carbon network and relative activity of their π electrons.[1,4] Gas sensors have been proposed as a result of their significant electronic conductance response to chemical environments. This remarkable structure-property relationship is used to engineer the graphene sheet through physical or chemical functionalization. Hydrogenation[4] and epoxidation[5] are two of the most noticeable approaches in this direction. Recently experimental studies have observed metal-semiconductor transition in graphene after hydrogenation,[4] which is recoverable through structural annealing. The reversible engineering on graphene has great potentials in designing functional nanoscale materials and devices. Controlling hydrogen binding on graphitic structure is also promising for the hydrogen storage industry, which provides high hydrogen storage weight ratio up to 7.7 wt %, to meet Department of Energy's 2010 goal (6 wt %). Further advances rely upon our understanding on the mechanism of tunable hydrogenation process. In this work, we address this problem from a combinational point of view from both structural and electronic aspects, i.e., to tune the hydrogenation of graphene by applying strain.

Experimental hydrogenation of graphene sheet can reach a high capacity and in a well periodic manner.[4,6] When the graphene monolayer is deposited or patterned on substrates, only one side of the graphene is accessible for hydrogenation.[7] The structure is called in *symmetric* phase [Fig. 1(a)]. On the other hand, if the graphene sheet is suspended or partially supported, the hydrogen atoms can be hosted on either side of the graphene sheets, i.e., in an *antisymmetric* phase [Fig. 1(b)]. In the second phase, binding carbon atoms at in A and B sublattices on opposite faces of graphene favors the total energy. The fully hydrogenated graphene with a C:H ratio of 1:1 is called graphane,[8,9] which will be discussed here.

The structures and properties of the graphene and graphane are investigated here through first-principles calculations. In our work, plane-wave basis sets based density functional theory is employed within local (spin) density approximation. We use the PWSCF code[10] for the calculation. We use Perdew–Zunger functional for the exchange-correlation energy, and ultrasoft pseudopotentials for the core-valence interactions. For all the results presented in this letter, energy cutoffs of 30 and 240 Rydberg are used for plane-wave basis sets and charge density grids, respectively. The settings are verified to achieve a total energy convergence less than 10^{-5} Ry/atom. For variable-cell relaxation, the criteria for stress and force on atoms is set to be 0.01 GPa and 0.001 Ry/Å. 16 Monkhorst–Pack *k*-points are used in each periodic direction for Brillouin zone integration, which is qualified for the energy convergence criteria of 3 meV.

The optimized structures of symmetric and antisymmetric graphane are shown in Fig. 1. In our calculation, a unit cell of graphane containing two carbon and two hydrogen atoms are used to represent crystalline graphene, with the in-plane lattice constant *a*. In comparison to pristine

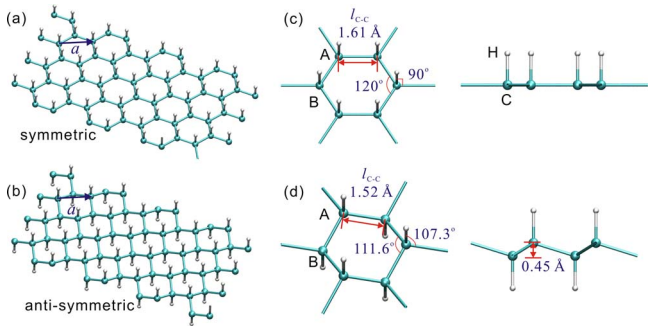

FIG. 1. (Color online) (a) and (b) Optimized structures of symmetric and antisymmetric graphane. The unit cell contains two carbon atoms (A and B denote the two sublattices) as in graphene and two hydrogen atoms. Panel (c) and (d) show the local atomic structures.

a)Author to whom correspondence should be addressed. Electronic mail: xuzp@mit.edu.

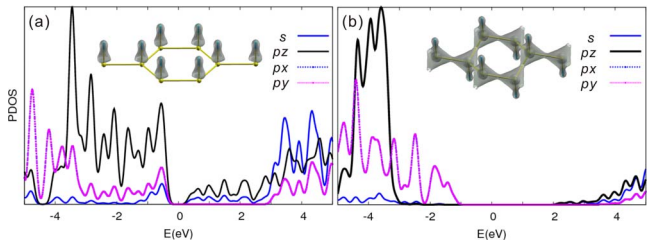

FIG. 2. (Color online) Density of states of graphane and its projection onto s, p_x, p_y, and p_z orbitals of carbon atoms. In symmetric phase (a), p_z state dominates the contribution near the Fermi energy (referred as 0 eV). The charge density as inset shows the π characteristic in the expanded graphene sheets. In antisymmetric phase (b), sp^3 hybridization removes the π characteristic and creates an energy gap of 3.35 eV. The inset shows sp^3 characteristic resembling the sp^3 bonds in diamond.

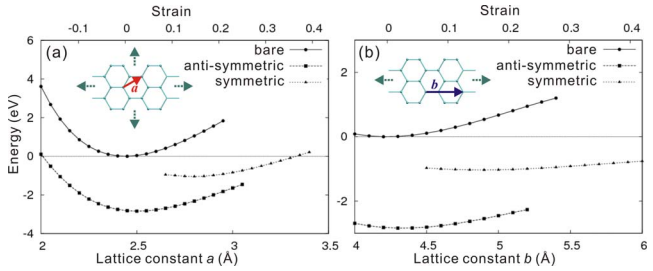

FIG. 3. (Color online) Energies of pristine graphene (with additional energy from isolated hydrogen atoms) and graphane under (a) biaxial and (b) uniaxial strain loading.

graphene where a_g=2.44 Å (consistent with experimental value 2.42 Å),[4] these two graphane phases have lattice constants a_{sym}=2.79 Å and a_{asym}=2.5 Å, respectively. The antisymmetric phase is found to be energetically (1.8 eV per carbon-hydrogen pair) more favorable than the symmetric one. Hydrogen atoms bound at two inequivalent carbon atoms in graphene lattice repulse each other and thus favor the configuration where adjacent carbon-hydrogen pairs reside at opposite surface of graphene sheet. Local structures of symmetric and antisymmetric graphane [Fig. 1(c) and 1(d)] show the characteristics of sp^2 (graphenelike) and sp^3 (diamondlike) features. In the symmetric phase, binding of hydrogen atoms expands the lattice constant underneath hexagonal graphene lattice by 14%, while preserving the planar configuration. As evidenced by localized density of states plot [Fig. 2(a)] near the Fermi level, the planar symmetry preserves sp^2 characteristic in graphane. Total density of states is projected onto s and p atomic orbital on each carbon atoms. p_z (l=1, m=0) orbital is distinct and contributes mostly near the Fermi level. Binding of hydrogen induces 0.14 electron transfer from hydrogen to carbon since carbon is slightly more electronegative than hydrogen. Also the hydrogenation through p_z orbital opens an energy gap E_g of 0.26 eV in comparison with the zero-gap nature of pristine graphene.

In antisymmetric phase, symmetry breaking between the two representative carbon (hydrogen) atoms in a unit cell allows the transition from sp^2 hybridization to sp^3 characteristics. The sp^3 hybridization induces out-of-plane corrugation of 0.45 Å and the carbon–carbon bond length is 1.52 Å, which is close to 1.54 Å in diamond. The bond angle A_{C-C-C}=111.6° and A_{H-C-C}=107.3° also resemble the tetrahedral angle 109° in diamond. The antisymmetric phase also opens a band gap E_g of 3.35 eV, which is smaller than that in diamond (4.2 eV from our calculation).

The abrupt change in lattice constant and planar structure of graphene after hydrogenation in symmetric and antisymmetric phase suggests possible control of the hydrogenation process and the properties of graphane through applying mechanical deformation. Pereira *et al.*[11] have shown that strain on graphene can change its electronic structure remarkably and thus provides a dimension for nanoelectronic engineering. We propose here to tune the hydrogenation process on graphene through strain engineering, i.e., by applying *a prior* deformation to graphene in prior to hydrogen binding or releasing. To quantify the binding strength between the hydrogen atoms and graphene sheet in terms of single carbon-hydrogen pair, we define the formation energy of graphane as $E_f=E_{graphane}-(E_{graphene}+E_H)$, where $E_{graphane}$ and $E_{graphene}$ are the energy of graphane and pristine graphene, respectively. The reference energy value for hydrogen E_H is set as −13.014 eV from spin-polarized calculation of isolated hydrogen atom. In absence of strain in the graphene lattice, symmetric and antisymmetric graphane phases have binding strength E_f of −1.044 and −2.847 eV per C–H atom pair.

The strain effects on the binding strength are investigated by applying biaxial in-plane strain before structural optimization. The results in Fig. 3 show energy of both the types of graphane structures, and also the combined system of pristine graphene and isolated hydrogen atom. The difference between the energy profiles at specific strain value is thus the binding energy E_f of hydrogen on graphene. Pristine graphene has an optimized lattice constant a_g=2.44 Å [Fig. 3(a)], while symmetric graphane has a_{sym}=2.79 Å. We investigate only the strain range where graphane structure is stable, i.e., the stress does not exceed its mechanical strength.

As shown in Fig. 3(a), The energy of both graphene (with additional constant energy terms from isolated hydrogen atoms) and symmetric graphane increases as the tensile strain is enhanced, When the lattice constant a exceeds 3.35 Å, the binding energy of symmetric graphane is larger than the value of undeformed system with pristine graphene and isolated hydrogen atoms. Also energy of nonhydrogenated system increases much faster than symmetric graphane. As a result, the binding energy of hydrogen is changed by 53.89% (with respect to the value without loading, a=2.44 Å) when the graphene is under a prestrain of 10% (from a=2.44 to 2.69 Å). The strain for sp^2 bond breaking in graphene is 18%, thus this strain is feasible as a reversible control. On the other hand, if the graphene sheet is restrained at a_g =2.44 Å against to in-plane expansion or the symmetric graphane is compressed from its equilibrium value to below 2.65 Å, repulsion between the carbon-hydrogen pairs will cause the hydrogenated structure to be mechanically unstable. The hydrogen atoms are repelled (released) from the graphene plane (Fig. 4). The sensitivity of symmetric hydrogenation of graphene on strain observed here thus provides a flexible and reversible controllability by simply stretching or compressing the graphene sheet.

In antisymmetric phase, a remarkable dependence of the formation energy on the strain is also observed [Fig. 3(a)]. Optimized lattice constant a_{asym}=2.5 Å. In-plane tensile and compressive strain of graphene sheet up to 10% can change the binding strength remarkably by 23.56% and −2.9%, respectively. The structure breaks at a tensile strain of 22% or

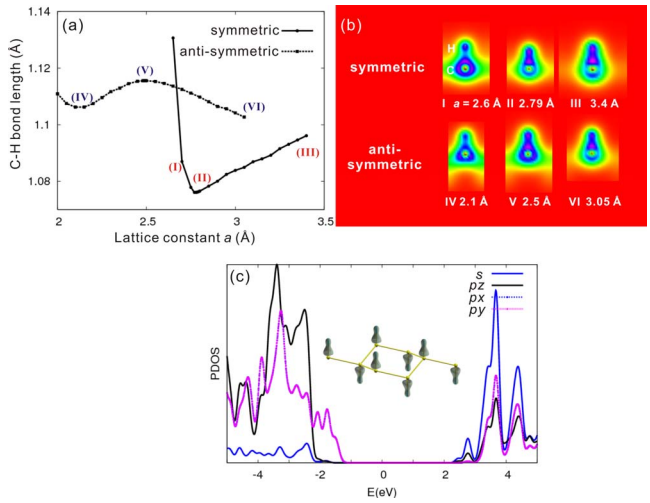

FIG. 4. (Color online) (a) Change in C–H bond length l_{C-H} under biaxial strain deformation. (b) Corresponding charge density distribution. (c) shows the density of states and charge density of antisymmetric graphane at an elongated lattice constant $a=3.05$ Å, where π characteristic of graphene is partially recovered.

a compressive strain of 26%. In comparison with symmetric phase, the strain modification of hydrogen binding energy is less significant as it has similar optimal lattice constant as pristine graphene. Under tensile strain, due to the weaker interaction between adjacent carbon-hydrogen pairs on the opposite sides of graphene, the expansion of in-plane lattice constant is found to be able to reduce its out-of-plane corrugation slightly and partially recover the π electron characteristics of graphene. Figure 4(a) shows the changes in carbon-hydrogen bond lengths l_{C-H} in these two phases. In symmetric phase, l_{C-H} increases at either tensile or compressive strain. As a is reduced to be less than 2.6 Å, the carbon-hydrogen bond is broken. Hydrogen atoms on graphene will be released from graphene sheet as discussed before. While at tensile strain and when the stress approaches the tensile strength and the in-plane sp^2 carbon network is about to be broken, l_{C-H} is elongated to the same value as in benzene or methane ($l_{CH\text{-methane}}=1.096$ Å). In antisymmetric phase, when tensile strain is applied, the planar configuration of graphene is partially recovered, suggesting emerging sp^2 feature. The carbon-hydrogen bond length decreases and approaches the value in sp^2 bonded symmetric phase in this situation. When antisymmetric structure is compressed, the sp^3 characteristic is enhanced and the carbon-hydrogen bond length also decreases toward the value in methane. As a result, the carbon-hydrogen bond length maximizes at the optimized lattice constant. As shown in Fig. 4(b), at an elongated lattice constant $a=3.05$ Å, the charge density distribution of antisymmetric phase of graphane resembles that of symmetric phases. This is also illustrated in Fig. 4(c) that shows the rising significance of p_z orbital, shifting toward the Fermi level. This sp^3-sp^2 changing in antisymmetric phase suggests that, as the distance between adjacent carbon-hydrogen pairs increases, the electronic coupling between the pairs that results in the sp^2-sp^3 transition from graphene to graphane is weakened.

The hydrogenation as a chemical functionalization of graphene not only modifies its electronic structure, but also affects mechanical property, as a result of sp^2 network change. Our results show that the in-plane modulus of graphene $C=d^2E/Ad\varepsilon^2=1260$ GPa is reduced by 52% and 26% in symmetric and antisymmetric phase, respectively, where E is potential energy, ε is in-plane biaxial strain and A is the calculated cross section area where the thickness of graphene is taken as 3.4 Å. Accordingly, the biaxial tensile strength has a strong reduction after hydrogenation, from 101.27 GPa to 49.64 and 67.92 GPa, due to the hydrogenation induced rehybridization.

The response of graphane structure under uniaxial loading is also investigated by applying uniaxial tension and relaxation of the unit cell length in the other direction, as shown in Fig. 3(b). Similar effects of strain modulation on the hydrogenation binding energy are observed, although the change is less significant as the lattice can be relaxed further in the transverse direction. The Young's modulus of graphene sheets $Y=1060$ GPa are found to be decreases by 77% and 25% in symmetric and antisymmetric phases. This also implicates that strain will introduce significant hydrogenation energy change in carbon nanotubes.[12]

In summary, we find remarkable mechanochemical effects on the basal-plane hydrogenation of graphene. The observations here suggest approaches for both graphene materials and devices engineering and hydrogen storage applications, with tunable and reversible controls from structural deformation.

[1]T. O. Wehling, A. I. Lichtenstein, and M. I. Katsnelson, Appl. Phys. Lett. **93**, 202110 (2008).
[2]L. A. Chernozatonskii, P. B. Sorokin, and J. W. Bruning, Appl. Phys. Lett. **91**, 183103 (2007).
[3]Z. Xu, Q.-S. Zheng, and G. Chen, Appl. Phys. Lett. **90**, 223115 (2007).
[4]D. C. Elias, R. R. Nair, T. M. G. Mohiuddin, S. V. Morozov, P. Blake, M. P. Halsall, A. C. Ferrari, D. W. Boukhvalov, M. I. Katsnelson, A. K. Geim, and K. S. Novoselov, Science **323**, 610 (2009).
[5]Z. Xu and K. Xue, Nanotechnology **21**, 045704 (2010).
[6]M. Z. S. Flores, P. A. S. Autreto, S. B. Legoas, and D. S. Galvao, Nanotechnology **20**, 465704 (2009).
[7]S. Ryu, M. Y. Han, J. Maultzsch, T. F. Heinz, P. Kim, M. L. Steigerwald, and L. E. Brus, Nano Lett. **8**, 4597 (2008).
[8]J. O. Sofo, A. S. Chaudhari, and G. D. Barber, Phys. Rev. B **75**, 153401 (2007).
[9]D. W. Boukhvalov and M. I. Katsnelson, Phys. Rev. B **77**, 035427 (2008).
[10]P. Giannozzi, S. Baroni, N. Bonini, M. Calandra, R. Car, C. Carlo, C. Davide, L. C. Guido, C. Matteo, D. Ismaila, C. Andrea Dal, G. Stefano de, F. Stefano, F. Guido, G. Ralph, G. Uwe, G. Christos, K. Anton, L. Michele, M.-S. Layla, M. Nicola, M. Francesco, M. Riccardo, P. Stefano, P. Alfredo, P. Lorenzo, S. Carlo, S. Sandro, S. Gabriele, P. S. Ari, A. Smogunov, P. Umari, and R. M. Wentzcovitch, J. Phys.: Condens. Matter **21**, 395502 (2009).
[11]V. M. Pereira and A. H. Castro Neto, Phys. Rev. Lett. **103**, 046801 (2009).
[12]A. Muniz, R. T. Singh, and D. Maroudas, Appl. Phys. Lett. **94**, 103108 (2009).